# **JAAS**



# PAPER View Article Online



Cite this: DOI: 10.1039/d2ja00170e

# An efficient method for high-precision potassium isotope analysis in carbonate materials

Xi-Kai Wang, Da Xiao-Ming Liu \*\* and Heng Chen \*\*D \*\*

High-precision potassium (K) isotope measurements in marine carbonates allow using this novel geochemical proxy to constrain seawater chemistry through geologic time. However, these measurements are still scarce due to the challenges of low-K contents in carbonates during K ion chromatography, such as insufficient sample purification, non-quantitative yield, and high accumulative blank. Here we optimize a dual-column K purification method that addresses these challenges, achieving a satisfactory K separation using 100–150 mg carbonates for routine high-precision K isotope analysis on the Sapphire<sup>TM</sup> MC-ICP-MS. We then report K isotope compositions in multiple certified reference materials, including limestone, dolostone, coral, and basalt for future inter-laboratory comparisons. The optimized K purification method provides great potential for future K isotope studies of marine carbonates.

Received 18th May 2022 Accepted 13th September 2022

DOI: 10.1039/d2ja00170e

rsc.li/jaas

#### 1. Introduction

Seawater composition reflects chemical exchanges between the lithosphere, hydrosphere, atmosphere, and biosphere. Among all elements investigated, K and its stable isotopes (39K and 41K) in seawater have been given particular attention, not only due to K being an essential nutrient for life,2-6 but also because K, a major cation in both Earth's crust (1.81%)7 and seawater  $(\sim 400 \text{ µg g}^{-1})$ , actively involves in various fluid-rock interactions between lithosphere and hydrosphere (e.g., silicate weathering;9-13 reverse weathering;14-17 hydrothermal alterations<sup>18-22</sup>). Recent high-precision measurements of potassium isotopes by multi-collector inductively coupled plasma mass spectrometer (MC-ICP-MS) have revealed significant 41K/39K variations in terrestrial samples, and a significantly higher  $\delta^{41}$ K value in seawater  $(\sim 0.12\%)^{23,24}$  relative to the bulk silicate Earth (BSE) ( $\sim$ -0.43\%<sub>00</sub>).<sup>25,26</sup> This could be explained by seawater K isotope mass balance, where major K sources (riverine and hydrothermal inputs) and sinks (reverse weathering and oceanic basalt alteration) in the ocean have a distinct magnitude of fluxes and isotopic signatures. 11,24,27 Therefore, records of the past K isotope composition in seawater should preserve information on how these sources and sinks change, providing key constraints on global K cycling over geological history.

Marine carbonates are one of the most important archives for seawater chemistry with regard to both elemental and isotopic compositions.<sup>28-31</sup> However, to date, limited studies have been carried out to explore the K isotope behavior in marine carbonates.<sup>32,33</sup> A major obstacle to such studies is that

<sup>a</sup>Department of Earth, Marine and Environmental Sciences, The University of North Carolina at Chapel Hill, Chapel Hill, NC, 27599, USA. E-mail: xiaomliu@unc.edu <sup>b</sup>Lamont-Doherty Earth Observatory, Columbia University, Palisades, NY, 10964, USA

the K isotope analysis in carbonate materials requires an efficient and high-yield pretreatment step to separate K from other matrix elements. Although a growing number of studies have developed cation-exchange chromatographic protocols for quantitative K purification (Table 1), the application for marine carbonates is challenging due to their low-K contents and high matrices (e.g., Ca and Mg). 27,34 To obtain enough K (e.g., 1 μg) for the high-precision isotopic analysis, more than 100 mg of carbonates are typically needed. For columns packed with resin volume less than 3 mL,35-39 this amount of loading exceeds their optimal capacity (i.e., 10% of the total column capacity), 40,41 therefore resulting in potential K loss and breakthroughs of matrix elements (e.g., Na, Mg, and Ca) into K collections. Alternatively, using columns with larger resin volume usually requires a larger volume of eluent (up to 300 mL),42 increasing total procedural blanks. Furthermore, changes in both K amount and K/matrix ratio can shift elemental elution curves. For example, Chen et al. 43 reported a dual-column K purification method for K-rich materials (i.e., silicate rocks, soils, and sediments) with high loading capacity and acceptable procedural blanks, however, their protocol cannot efficiently exclude excessive Mg from carbonates. Repetition of their columns will nevertheless increase the accumulative blank. As such, a robust K chromatography suitable for low-K marine carbonates with low blank and high yield is needed.

In this study, we present an efficient dual-column K purification protocol for marine carbonates to achieve high-precision K isotope measurements using a Sapphire  $^{\text{TM}}$  MC-ICP-MS. The first column was modified based on Chen *et al.* <sup>43</sup> through optimization of the K elution range under various amounts of carbonate loading. The second column was developed using a synthetic solution, certified references, and carbonate samples aiming for a better K separation. We tested the yield and procedural blank of

 Table 1
 Potassium ion-exchange separation procedure comparison (modified after Wang et al.<sup>27</sup>)

	Strelow et al. 55	Humayun and Clayton <sup>42</sup>	Wang and Jacobsen <sup>25</sup>	Li <i>et al.</i> <sup>56</sup>	Morgan et al. <sup>57</sup>	Hu et al. 38	Chen et al. <sup>43</sup>	Li et al.³⁵	Chen et al. <sup>47</sup>	Huang et al. <sup>39</sup>
Number of columns	1	1	1	2		1	2	1	1	1
Sample weight	$\sim$ 1 g	$\sim$ 1 g	$\sim$ 10–50 mg	10–50 mg	$\sim\!\!20~{ m mg}$		$\sim$ 10–100 mg	$\sim$ 50 mg	<20 mg	10–20 mg
Resin	Bio-Rad AG50W-X8 (200–400 mesh)	Bio-Rad AG50W-X8 (100–200 mesh)	Bio-Rad AG50W-X8 (100–200 mesh)	Bio-Rad AG50W-X12 (100–200 mesh)	Dionex CS-16 cation exchange column	Bio-Rad AG50W-X8 (200–400 mesh)	Bio-Rad AG50W-X8 (100–200 mesh)	Bio-Rad AG50W-X8 (200– 400 mesh)	Bio-Rad AG50W-X8 (200–400 mesh)	Bio-Rad AG50W-X8 (200–400 mesh)
Column type	Borosilicate glass	Pyrex or quartz	Quartz	Quartz		Bio-Rad poly- prep polyethylene column	Poly-prep econopac polyethylene column	Savillex PFA micro-column	Bio-Rad poly- prep polyethylene column	Quartz
Diameter	2.5 cm	2.2 cm	1 cm	0.4 cm		0.8 cm	1.5 cm	4 mm		7 mm
Resin volume	90 mL	90 mL	13 mL	1 mL		2 mL	17 mL	2.3 mL	2 mL	2.7 mL
Cleaning	$_3$ M HNO $_3$	4 M HNO <sub>3</sub> or 6 M HCl	4 M HCl	$4.5 \mathrm{~M~HNO_3}$		$6 \text{ M HCl } + $ $H_2\text{O} + $ $1 \text{ M HNO}_3$	6 M HCl	$6 M HCl + H_2O$	6 M HCl	$6 \text{ M HCl } + \text{H}_2\text{O}$
${\rm Max\ capacity}^a \\ {\rm (mEq)}$	153	153	22.1	2.1		3.4	28.9	3.9	3.4	4.6
Eluting	$0.5~\mathrm{M~HNO_3}$	$0.5 \mathrm{~M~HNO_3}$	$0.5 \mathrm{~M~HNO}_3$	$1.5~\mathrm{M~HNO_3}$	$0.2\%~\mathrm{HNO_3}$	$0.5~\mathrm{M~HNO_3}$	$0.7~\mathrm{M~HNO_3}$	2 M HCl + 0.1 M HF	0.45 M HCl	$0.5~\mathrm{M~HNO_3}$
Potassium fraction	600–850 mL	700–1000 mL	180–340 mL	5-17 mL		14-36 mL	88–195 mL	12–22 mL	20–45 mL	25-49 mL
Recovery Blank	0.5-1	≥99.8%	>99%	$99.4 \pm 2.1\%$	0.06-1.06%		>99% 0.26 + 0.15 us	$99.5 \pm 0.6\%$	>99%	10 50
DIAIIK	8μ 1–c.o	0.2%	0.02 µg	3-o 11g	0.00-1.00%		gh c1.0 ± 02.0	<10 IIS	Sm cr.o	10 IIS

the newly developed K purification method, and we successfully applied this method to three well-studied carbonate references, one dolostone sample, and one silicate standard.

### 2. Experimental methods

#### 2.1 Chemicals and samples

Ultra-pure water with a resistivity of 18.2 M $\Omega$  was produced using a Milli-Q purification system (Direct-Q® 3 UV, Merck Millipore<sup>TM</sup>, Germany). Nitric acid (HNO<sub>3</sub>), hydrochloric acid (HCl), and hydrofluoric acid (HF) were distilled twice from ACS Grade using a Savillex<sup>TM</sup> DST-1000 still. Double-distilled HNO<sub>3</sub> and HCl were diluted with Milli-Q water to the required concentrations.

To optimize the K separation, we investigated three in-house carbonate samples: a limestone sample from Key Largo (KL Cal), a dolostone sample from the South China Sea (SCS Dol), and a bivalve mollusk Atrina rigid. The limestone and dolostone samples consist of pure calcite and dolomite, respectively. Their sampling information and elemental concentrations have been reported in the literature.44,45 The bivalve was collected by Prof. Joseph G. Carter from Sanibel, Florida. About 62 g calcite shell was cleaned by ultra pure water (Milli-Q) before being dried and then powdered by a Spex Certiprep® ball mill at the University of North Carolina at Chapel Hill (UNC-CH). We also used three certified carbonate reference materials: a limestone standard (NIST SRM 1d) was obtained from the National Institute of Standards and Technology (NIST), while a coral (JCp-1) and a dolostone standard (JDo-1) were obtained from the Geological Survey of Japan (GSJ). One basalt standard (BHVO-2) was also included to monitor the accuracy of the K isotope analysis.

In addition, we mixed single-element ICP-MS standards (Inorganic Ventures  $^{\rm TM}$ , USA) to prepare a synthetic solution, containing 7460  $\mu g\,g^{-1}$  Na, 4943  $\mu g\,g^{-1}$  Mg, 4675  $\mu g\,g^{-1}$  K, 4497  $\mu g\,g^{-1}$  Ca, 1924  $\mu g\,g^{-1}$  Ti, 96  $\mu g\,g^{-1}$  V, 75  $\mu g\,g^{-1}$  Cr, 1019  $\mu g\,g^{-1}$  Fe, and 256  $\mu g\,g^{-1}$  Rb in 2% (v/v) HNO $_3$ . The elemental compositions were determined by taking the maximum concentration of each element in the residues of the studied carbonates after the first column. The mixed solution aims to emulate the matrix residue of carbonate samples after the first column and to test the separation of the second column.

#### 2.2 Sample preparation

To achieve total dissolution,  $\sim$ 50–250 mg of carbonate powder samples were pretreated with 30%  $H_2O_2$  (Optima grade, Fisher)

Table 3 Parameters of the second columns and K elution ranges

Resin	Column length (cm)	Elution acid	K fraction (mL)
AG50W-X8 (100–200 mesh)	13	0.3 M HNO <sub>3</sub>	80-140
AGSOW AS (100 200 mesh)	13	0.4 M HNO <sub>3</sub>	60-100
	17	0.4 M HNO <sub>3</sub>	65-105
	13	0.5 M HNO <sub>3</sub>	45-85
	17	0.5 M HNO <sub>3</sub>	50-95
	13	0.7 M HNO <sub>3</sub>	25-65
	13	$1.0 \text{ M HNO}_3$	15-45
	13	0.5 M HCl	40-90
	13	1.0 M HCl	15-50
AG50W-X12 (200–400 mesh)	13	$0.5 \text{ M HNO}_3$	$125-^{a}$
	13	$0.7 \text{ M HNO}_3$	85-135
	13	$1.0 \text{ M HNO}_3$	50-85
	13	0.5 M HCl	$125-^{a}$
	13	1.0 M HCl	50-90

<sup>&</sup>lt;sup>a</sup> Potassium was not totally washed out when the experiment stopped.

to remove organics before being digested through a three-step protocol: the samples were first digested with an HF–HNO $_3$  (3:1, v/v) mixture on a hot plate at  $\sim$ 150 °C overnight. After the samples were evaporated to dryness, the residues were then treated with *aqua regia* on a hot plate at  $\sim$ 150 °C to achieve total dissolution. Finally, the samples were dried down and redissolved in 2 mL 0.7 M HNO $_3$  for chromatography. Apart from the carbonates, 1 mL synthetic solution was evaporated and redissolved by acid before being loaded onto the second column. All sample preparation was performed using Savillex<sup>TM</sup> Teflon beakers in a class 100 laminar flow exhaust hood (AirClean® 600 PCR workstation) at the Plasma Spectrometry (PMS) Laboratory at UNC-CH.

#### 2.3 Cation exchange chromatography

A dual-column chromatography was optimized for the purification of K from carbonate matrices. The first column is used to separate K from the major carbonate matrix, and the second smaller column is able to further remove residual impurities from K.

We optimized the loading amount and calibrated the K elution range for the first column of Chen *et al.*<sup>43</sup> The columns were prepared using Bio-Rad<sup>TM</sup> Econo-Pac columns (1.5 cm ID,

Table 2 Experimental design for the optimization of the first column

Sample name	Sample weight (mg)	Cation load <sup>a</sup> (mEq)	Mg <sup>2+</sup> mass load (mg)	Ca <sup>2+</sup> mass load (mg)	K <sup>+</sup> mass load (ng)
SCS Dol	106.6	2.31	10.97	21.44	2669
	150.9	3.27	15.53	30.35	3779
	203.1	4.41	20.90	40.85	5086
	253.5	5.50	26.09	50.99	6348
KL Cal	106.6	2.13	0.25	43.06	1604
	207.0	4.14	0.49	83.63	3115

<sup>&</sup>lt;sup>a</sup> Cation load has been calculated assuming all samples are pure carbonates.

Table 4 Experimental design and results for the second column

Sample type	Sample name	Sample weight (mg)	K concentration $(\mu g g^{-1})$	K <sup>+</sup> mass load (μg)	K elution range (mL)	K recovery (%)	Rb/K (%)
Limestone	NIST SRM 1d (1)	31.6	1174.5	37.1	65-100	100.0	0.10
	NIST SRM 1d (2)	40.9		48.0	60-100	100.0	0.18
	NIST SRM 1d (3)	47.9		56.3	60-100	100.0	0.29
	NIST SRM 1d (4)	105.6		124.0	60-100	100.0	0.27
	KL Cal	115.0	15.1	1.7	65-100	99.7	0.20
	In-house bivalve	122.7	100.4	12.3	60-90	100.0	0.03
Aragonite	JCp-1	107.9	188.7	20.4	65-95	100.0	0.07
Dolostone	SCS Dol	108.6	25.1	2.7	65-95	100.0	0.09
	JDo-1	109.1	20.9	2.3	65-90	100.0	0.24
Basalt	BHVO-2	39.4	4545.3	179.1	60-100	100.0	0.05

 $\begin{tabular}{lll} \textbf{Table 5} & Overview of the developed K isotope chromatographic procedure \\ \end{tabular}$ 

First column purification	17 mL Bio-Rad AG50W-X8 (100–200 mesh) in Bio-Rad Econo-Pac column (1.5 cm ID)			
Step	Solution	Volume (mL)		
Cleaning	6 M HCl	100		
Conditioning		60		
Loading sample		2		
Matrix elution	$0.7 \text{ M HNO}_3$	75		
Pre-cut 1		5		
K collection		80		
Post-cut 1		5		
Post-cut 1 Second column purification	6.5 mL Bio-Rad A 200 mesh) in cus polypropylene co	AG50W-X8 (100–		
	200 mesh) in cus	AG50W-X8 (100– etomized		
Second column purification	200 mesh) in cus polypropylene co	AG50W-X8 (100– stomized lumn (0.8 cm ID)		
Second column purification Step	200 mesh) in cus polypropylene co Solution	AG50W-X8 (100– stomized lumn (0.8 cm ID) Volume (mL)		
Second column purification Step Cleaning	200 mesh) in cus polypropylene co Solution	AG50W-X8 (100– stomized lumn (0.8 cm ID) Volume (mL)		
Second column purification Step Cleaning Conditioning	200 mesh) in cus polypropylene co Solution	AG50W-X8 (100– etomized lumn (0.8 cm ID) Volume (mL)		
Second column purification Step Cleaning Conditioning Loading sample	200 mesh) in cus polypropylene co Solution	AG50W-X8 (100– stomized lumn (0.8 cm ID) Volume (mL) 20 20 10		
Second column purification Step Cleaning Conditioning Loading sample Matrix elution	200 mesh) in cus polypropylene co Solution 6 M HCl Milli-Q water	AG50W-X8 (100– ctomized lumn (0.8 cm ID) Volume (mL) 20 20 10 1		
Second column purification Step	200 mesh) in cus polypropylene co Solution 6 M HCl Milli-Q water	AG50W-X8 (100- ctomized lumn (0.8 cm ID) Volume (mL) 20 20 10 1 55		

polypropylene) packed with 17 mL Bio-Rad<sup>TM</sup> precleaned AG50W-X8 (100–200 mesh) resin. Columns were first cleaned with 100 mL 6 M double-distilled HCl to remove impurities and conditioned with 60 mL 0.7 M HNO $_3$ . Then various amounts of the KL Cal and SCS Dol covering a wide spectrum of marine carbonate matrices (Table 2) were loaded onto the columns and eluted using 0.7 M HNO $_3$ . Each 5–10 mL eluent was collected continuously. A total of 190 mL was collected for each sample. All elution cuts were evaporated and dissolved in 2% (v/v) HNO $_3$  for ICP-MS analysis.

A suite of experiments was carried out using a synthetic solution to optimize chromatographic parameters for the second column, which is built on a customized polypropylene

column (0.8 cm ID). Table 3 gives a summary of column parameters tested, including resin type, column length (aspect ratio), acid type, and acid molarity. In general, the column was pre-cleaned with 20 mL 6 M HCl and 20 mL Milli-Q water before being conditioned with acid. After conditioning, 1 mL synthetic solution was loaded onto the column, and eluents were collected per 5 mL for elemental analysis until K was eluted out completely. Acids used for conditioning, loading, and elution were kept the same. A parallel study was also performed using the same synthetic solution on the second column by Chen et al.43 for comparison. The K separation of the optimized second column was further tested by certified references and natural carbonate samples (Table 4). We selected  $\sim$ 30-100 mg high-K samples (i.e., NIST SRM 1d, BHVO-2) with K ranging from  $\sim$ 37 to 179 µg to evaluate the influence of the amount of loaded K and other matrix cations on the separation of our method. The rest low-K carbonates weighing within the optimal loading amount of the first column (100-150 mg) were also investigated aiming to obtain enough K (>1 µg) for isotopic analysis. These samples were passed through the first column before being loaded onto the second column to obtain the calibration curves. K recoveries were monitored throughout the procedure.

Finally, we applied the developed dual-column protocol (Table 5) to isolate K from four certified references NIST SRM 1d, JCp-1, JDo-1, BHVO-2, and one in-house South China Sea dolostone sample. We also tested the procedural blanks four times using four different columns following the same protocol. The method is detailed as follows. After loading the sample on the first column, 75 mL of 0.7 M HNO3 was added to elute the matrix elements, followed by another 5 mL 0.7 M HNO3 collected into a 7 mL SavillexTM beaker as the pre-cut. K was eluted by adding 80 mL 0.7 M HNO<sub>3</sub> before a 5 mL post-cut was collected. The K collection was evaporated, redissolved in 0.4 M HNO<sub>3</sub>, and then loaded onto the second column. K fraction was collected between 60-100 mL. 5 mL pre-cut and post-cut were collected before and after the K fraction, respectively. All precuts and post-cuts from two steps of the column, as well as the K fraction of each sample, were measured with a Q-ICP-MS (Agilent<sup>TM</sup> 7900) to monitor the recovery. The recovered K was dried down and redissolved with 2% (v/v) HNO3 for isotopic analysis using a Sapphire™ MC-ICP-MS.

#### 2.4 Instrumental analysis

To obtain elution curves for both first and second columns, the elution cuts were analyzed using an Agilent<sup>TM</sup> 7900 quadrupole ICP-MS (Q-ICP-MS) at the PMS Lab, UNC-CH. Samples in 2% (v/v) HNO<sub>3</sub> were calibrated using matrix-matched multi-element standards before being measured under helium cell mode to reduce interferences. An internal standard solution containing 100 ng g<sup>-1</sup> of Be, Ge, In, and Bi was used to correct for the instrumental drift. A river water standard SLRS-6 obtained from the National Research Council of Canada was measured routinely, yielding a long-term accuracy of  $\sim$ 5% for major elements, compared with certified values and the GEOREM database.<sup>46</sup>

All K isotopic analyses in this study were conducted following the method by Chen et al.47 using a Nu Instruments Sapphire<sup>TM</sup> MC-ICP-MS (SP004) in the Novel Isotopes in Climate, Environment, and Rocks (NICER) Laboratory at the Lamont-Doherty Earth Observatory, Columbia University. Potassium isotope ratios (41K/39K) were determined using the standard-sample bracketing method. Samples and standard NIST SRM 3141a were diluted to 150  $\pm$  1.5 ppb K solutions in 2% (v/v) HNO<sub>3</sub> for analysis. K solutions were introduced into a "dry plasma" through the Apex Omega desolvating nebulizer (ESI $^{\text{TM}}$ ), and  $^{39}$ K and  $^{41}$ K signals were measured by Faraday cups equipped with  $10^{10}~\Omega$  and  $10^{11}~\Omega$  resistors, respectively. The Sapphire™ MC-ICP-MS is equipped with a collision cell where He and H2 work as collision gas and reaction gas respectively, to minimize the isobaric interferences of Ar<sup>+</sup> and ArH<sup>+</sup>, so that potassium isotope signals can be directly measured on the peak center with a 1300 W RF power in low resolution mode. Prior to

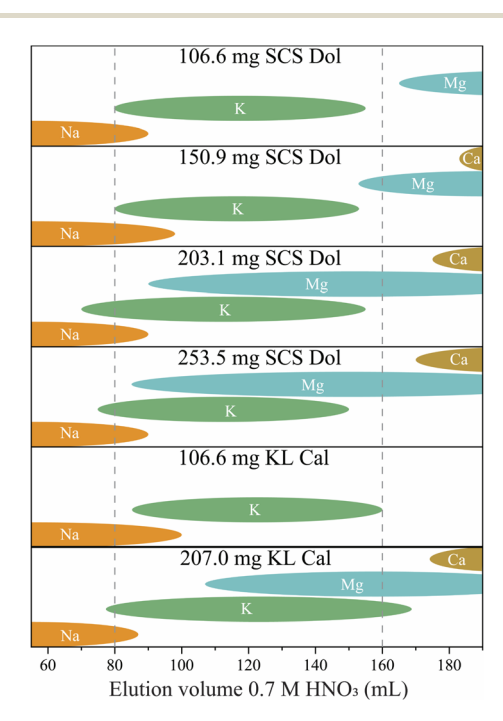


Fig. 1 Elution profiles for  $\sim$ 100–250 mg KL Cal and SCS Dol *via* the first column of Chen *et al.*<sup>43</sup> Elution profiles are shown by conceptual bubbles. Two ends of a bubble indicate the elution fraction range.

each analysis, a 20 s on-peak acid blank was measured and subtracted from the analyte signal, and a typical signal for 150 ppb  $^{39}{\rm K}$  could reach as high as  $\sim\!165$  V. Mass 40 was constantly monitored for Ca level as  $^{40}{\rm CaH}^+$  directly interferes with  $^{41}{\rm K}^+$ . Each analysis consisted of 45 cycles of 4 s integrations and took  $\sim\!100$  ng K. Analyses were repeated at least four times for all samples in this study. Their K isotope data are reported in  $\delta^{41}{\rm K}$  relative to the standard NIST SRM 3141a:

$$\delta^{41} K(\%) = \left\{ \frac{\binom{4^1 K}{3^9 K}}{\binom{4^1 K}{3^9 K}}_{\text{sample}} - 1 \right\} \times 1000$$

The long-term external reproducibility of better than 0.07% (2SD) was obtained based on the replicate analyses of a seawater sample.<sup>47</sup>

#### Results and discussion

#### 3.1 Optimization of the first column

The first column is designed to separate K from major elements (e.g., Na, Al, Mg, and Ca) in carbonate samples. Its original protocol by Chen et~al. has been extensively applied to extract K from  $\sim \! 10 - \! 100$  mg silicates for isotopic analysis.  $^{12,13,17,20,48}$  However, it is not suitable for low-K carbonates due to remarkably high Ca and/or Mg in the matrix. Such matrices will cause significant elemental peak shifts, leading to unsatisfactory K separation.

Elution profiles of Na, Mg, K, and Ca obtained for the first column calibrated with a KL calcite and a SCS dolostone are listed in Table 2 and shown in Fig. 1. We note here that elution profiles are shown by the bubbles instead of the elution curves in percentage since they can provide more accurate elemental elution ranges (see discussion in Section 3.2). For all the samples tested, increasing the column load shifts K elution peaks leftwards and increases the K elution width. K is consistently eluted from 80 to 160 mL when the column is loaded with dolomite less than 150 mg, whereas a small amount of K can be observed in the cuts prior to 80 mL with a larger loading amount. A similar K elution pattern is also observed in 200 mg calcite, where K is collected in elution cuts before 80 mL and after 160 mL.

High Mg concentrations in carbonates especially in dolostones make it difficult to separate K from Mg. Calibration results show that higher loading cation quantity leads to more Mg breakthroughs into K fractions (Fig. 1), and satisfactory K separation can only be achieved with less than 150 mg carbonate. Overlaps between Mg and K observed for 200 mg and 250 mg dolomite yield Mg/K ratios of 646 (ng ng<sup>-1</sup>) and 7283 (ng ng<sup>-1</sup>), respectively, in K fractions. Such an amount of Mg necessitates repeated columns, which, however, may introduce non-trivial contamination from the eluent given the low K abundance in carbonate. The presence of excessive Mg may also cause a matrix effect that results in inaccurate K concentration measurements on Q-ICP-MS.

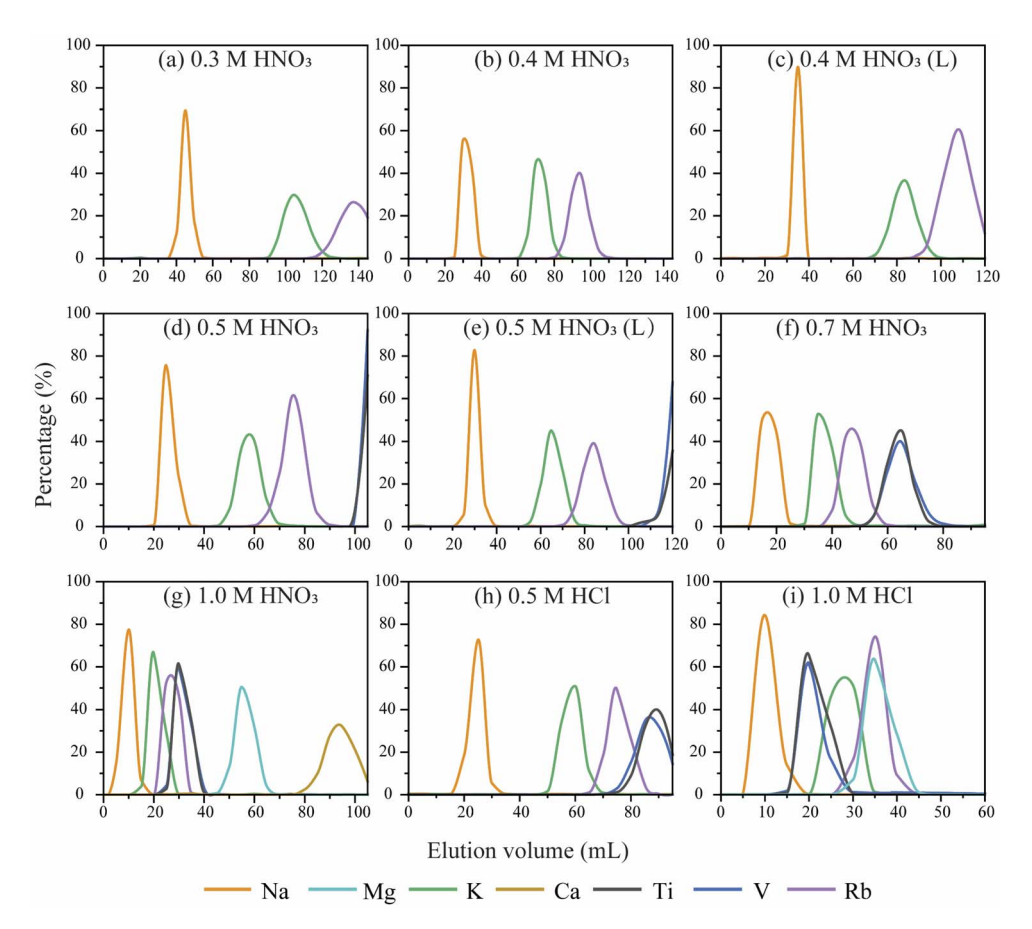


Fig. 2 Elution curves for the synthetic solution with different eluents on AG50X8 resin (100-200 mesh). L indicates a longer column (17 cm).

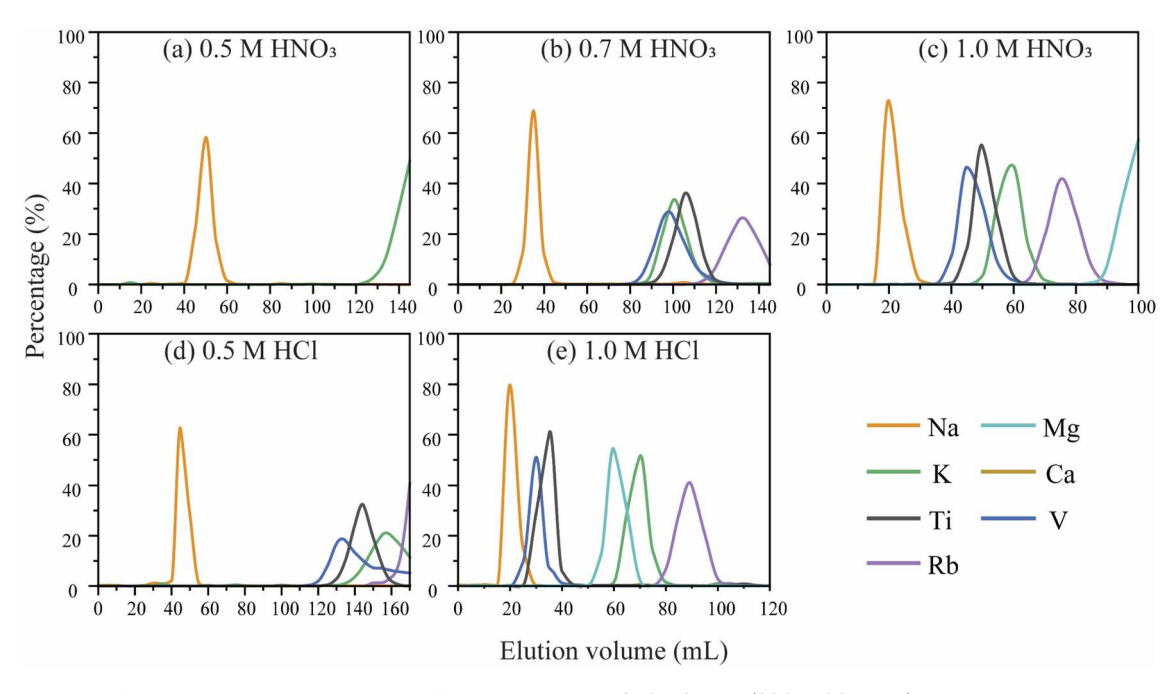
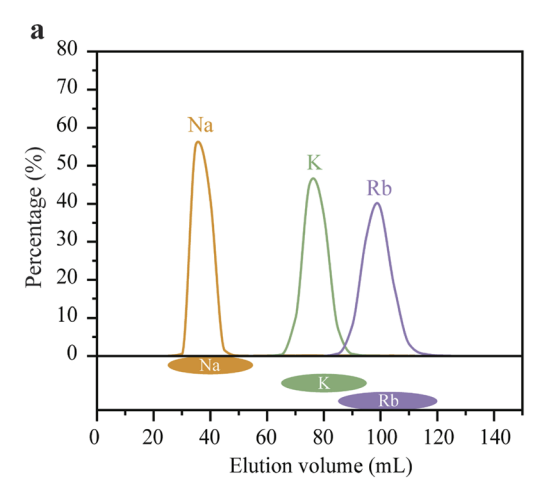


Fig. 3 Elution curves for the synthetic solution with different eluents on AG50X12 resin (200-400 mesh). L indicates a longer column (17 cm).

Paper JAAS



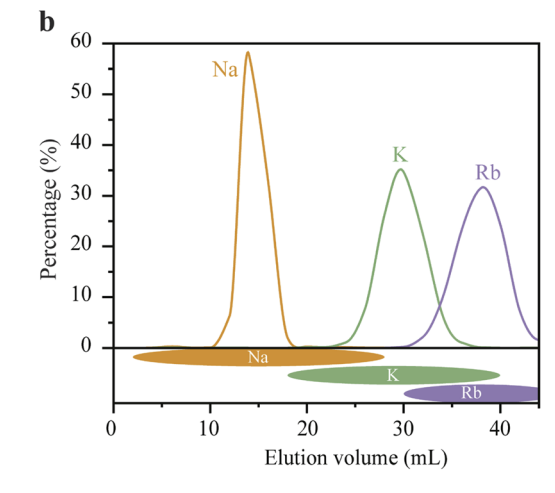


Fig. 4 Elution profiles of the synthetic solution using (a) the second column developed in this study and (b) the second column in Chen *et al.*<sup>43</sup> are shown by elution curves (upper panel) and conceptual bubbles (lower panel). Two ends of the bubble indicate the accurate elution range of the cation.

Calcium can be completely separated from K using the first column, regardless of the loading amount and mineralogy. This is important because K isotope measurement can be significantly shifted by CaH<sup>+</sup>.<sup>47</sup> In contrast, breakthroughs of Na into K fractions are unavoidable during the first column. Similar distribution coefficients of Na and K decrease the separation effectiveness of the first column.<sup>49</sup>

In summary, 100–150 mg carbonates are preferred for the first column for their consistent K elution range and effective separation from most matrices. K recoveries after the column optimization were nearly 100% ensuring no on-column isotopic fractionation. Nevertheless, the application of the first column cannot achieve complete K isolation in observance of the small amount of residual Na and Mg, as well as trace elements including Rb, V, and Ti collected in the K fraction. Hence, an additional second column is needed for further purification. All samples used for the subsequent column development were kept under 150 mg.

#### 3.2 Development of the second column

Bio-Rad™ AG50W-X8 resin (100-200 mesh) with an 8% crosslink is commonly used in existing K chromatographic procedures (Table 1). AG50W-X12 (200-400 mesh) resin is expected to have a larger loading capacity and better separation resolution due to its larger crosslink rate (12%) and total surface area.<sup>50</sup> Therefore, both resins were loaded in an identical column (0.8 cm ID), and calibrated using the same synthetic solution (Table 3). Calibration results present two advantages of X8 resin over X12 resin (Fig. 2 and 3). First, the column packed with X8 resin has a shorter elution duration of K separation using the same acid. For example, a 60 mL K peak gap is found between X8 (25–65 mL, Fig. 2f) and X12 resin (85–135 mL, Fig. 3b) when 0.7 M HNO<sub>3</sub> is the eluent. A similar gap can also be found for 1 M HCl, where X8 and X12 resins have K peaks ranging from 15 to 50 mL and 50 to 90 mL (Table 3), respectively. Second, the application of X12 resin is limited by V and Ti overlapping with

K (Fig. 3). Although X12 resin eluted by 0.5 M HNO $_3$  seems to sufficiently isolate K (Fig. 3a), the K retention time is more than 12 h.

Elution profiles of the mixed solution were obtained for X8 resin with HNO<sub>3</sub> and HCl (Fig. 2). For both acids, less concentrated acid can spread out the elemental peaks, thereby coelution matrix can be effectively eliminated. Among all the elution acids, 0.4 M HNO<sub>3</sub> is preferred due to the following reasons: (1) no Na, V, Ti, Mg, and Ca were collected in the K fraction; and (2) K elution range is 60–100 mL, the separation work can be finished in about 8 h at the elution rate of 0.2 mL min<sup>-1</sup>. A previous study suggested using a larger aspect ratio column to improve the separation efficiency.<sup>51</sup> However, such improvement is negligible in the long column (17 cm) tested in this study (Fig. 2c and e) and a significantly longer retention time is present.

We also loaded 1 mL mixed solution onto the second column by Chen et al.43 for comparison. The results are shown by both "bubbles" and elution curves (Fig. 4). We found that the overlap between elements in the bubble figure is sometimes unidentifiable in the elution curves, because the small tails at both ends of the elution curves could be shaded by the major peak. Here we note that although elution curves can provide the elution order and the curve tailing, they cannot provide the accurate elution range and the separation effectiveness, especially for columns loaded with heavy matrix materials. The elution curves of our second column are consistent with the bubble figure that no Na was collected in the K fraction (Fig. 4a). However, Na breakthrough into the K fraction can be observed in the second column by Chen et al.,43 even though elution curves show no overlap (Fig. 4b). Compared with Na, Rb cannot be completely removed using both columns. Yet Rb is not problematic for our column due to its low content in natural carbonates (see discussion below).

Potassium was chromatographically isolated from certified references and natural carbonate samples (Table 4). First, the samples were passed through the first column, during which no

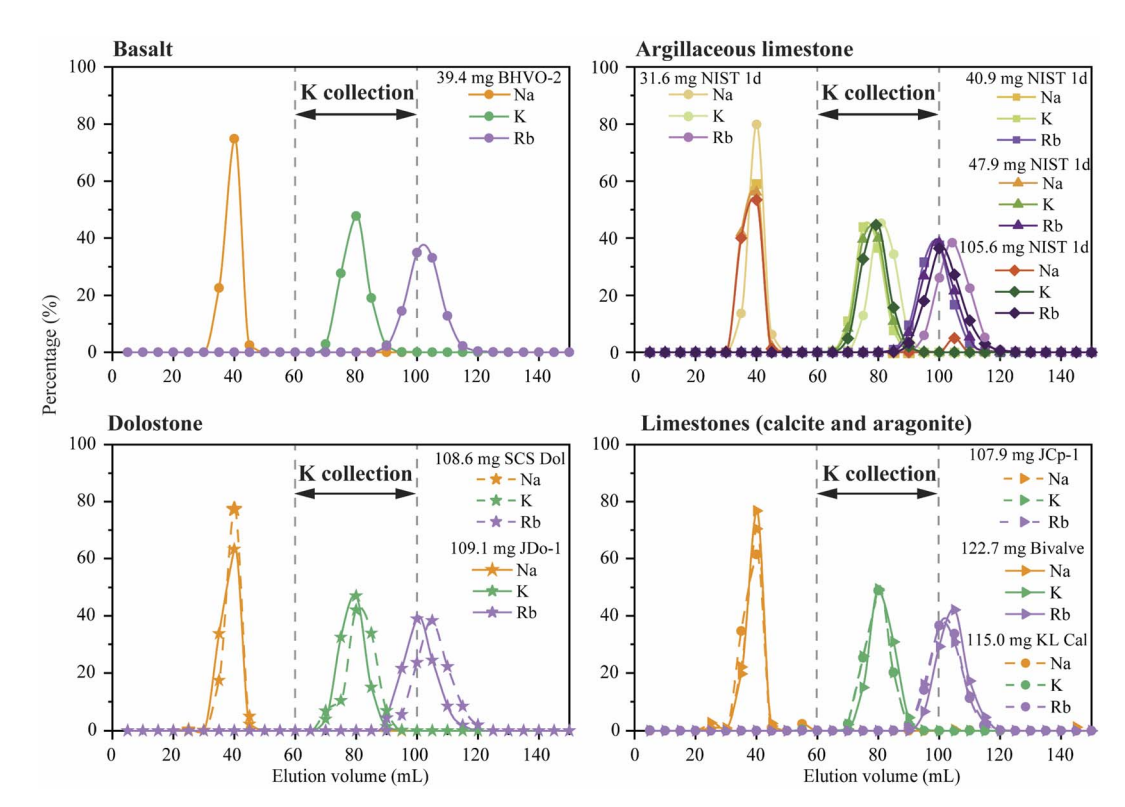


Fig. 5 Elution curves of natural carbonates and reference materials *via* the second column separation after the first column purification. The K elution range (bracketed by the grey dashed line) is 60–100 mL. Na is absent in K fractions, Rb/K is less than 0.3%.

K loss was found. The K cuts were then loaded onto the second column to get the calibration results (Fig. 5). With loaded  $K^+$  ranging from 1.7 to 179.1  $\mu$ g, K peaks constantly fall into 60–100 mL, consistent with the elution range obtained using the synthetic solution. In addition, a 5–20 mL elution gap between

Na and K ensures the total K recovery without Na. And for all the samples tested, Rb/K ratios were always less than 0.3% after the columns (Table 4). Such impurities will not compromise the accuracy of K isotope measurement,<sup>47</sup> so we do not need to repeat this column. Furthermore, our newly developed dual-

Table 6 K isotope compositions in certified reference materials

Sample name	Sample type	$\delta^{41} \mathrm{K} \left( \%_{oo} \right)$	2SD	N	Data source
BHVO-2	Basalt	-0.50	0.19	4	Li et al. <sup>37</sup>
		-0.43	0.06	5	Hu et al. <sup>38</sup>
		-0.46	0.04 (2SE)	13	Chen et al. 43
		-0.47	0.03 (2SE)	79	Chen et al. 12
		-0.40	0.04	6	Li et al. <sup>35</sup>
		-0.48	0.04	7	Li et al. <sup>17</sup>
		-0.47	0.03	26	Chen et al.47
		-0.434	0.04	11	Moynier et al.58
		-0.41	0.03	6	This study
NIST SRM 1c	Limestone	-0.58	0.03 (95% C.I.)	14	Chen et al. 43
NIST SRM 1d	Limestone	-0.65	0.09 (95% C.I.)	8	Li et al. <sup>33</sup>
		-0.60	0.02	6	This study
		-0.57	0.04	4	This study
JCp-1	Aragonite	-0.20	0.07 (95% C.I.)	_	Li et al. <sup>32</sup>
		-0.10	0.10 (95% C.I.)	8	Li et al. <sup>33</sup>
		-0.31	0.02	6	This study
JDo-1	Dolostone	-1.00	0.01	6	This study
		-1.00	0.01	6	This study
SCS Dol	Dolostone	-0.49	0.02	4	This study
		-0.48	0.03	4	This study
		-0.50	0.01	6	This study

column method yields satisfactory K recovery of nearly 100% (Table 4) without any isotopic fractionation during the column chemistry.

The average of the four total procedure blanks for the entire K purification process is 29.5  $\pm$  4.4 ng (2SD; n = 4), which is about 9 times lower than that of Chen et al. 43 (0.26  $\pm$  0.15 µg, 2SD, n = 7). In our study, KL calcite has a minimum K of 1.73 µg, yielding a sample/blank ratio of 59. Assuming the blank has the  $\delta^{41}$ K value of -1.31%, 43 the blank will introduce an error of  $\sim$ 0.02\%, which is below the analytical uncertainty of K isotope measurement. Therefore, the blank is negligible for all samples tested in this study. The whole experimental process generally takes 2 days, including all the column and evaporation steps. Although our method does not significantly reduce the experimental time, our method is more efficient than existing dualcolumn protocols because their protocols need repeated separation for low-K carbonates either to eliminate matrices or to obtain enough K (i.e., 1 μg) for isotopic analysis using MC-ICP-MS.27

#### 3.3 The K isotope composition of reference materials

We report potassium isotope compositions of the following materials: BHVO-2 (basalt), NIST SRM 1d (limestone), JCp-1 (coral), JDo-1 (dolostone), and SCS dolostone to evaluate the reproducibility of our newly developed chromatographic method and to facilitate inter-laboratory comparison (Table 6). Basalt BHVO-2 is one of the most extensively used geological standards. Therefore a BHVO-2 sample was processed and analyzed using our method, its K isotope value ( $-0.41 \pm 0.03\%$ ) n = 6) is in good agreement with previous studies. This validates the analytical accuracy of this study, and also implies the potential of our method in dealing with other low-K samples beyond carbonate (e.g., ultramafic rocks). The K isotope compositions of two NIST SRM 1d are  $-0.60 \pm 0.02\%$  (2SD, n =6) and  $-0.57 \pm 0.04\%$  (2SD, n = 4), respectively. The results are consistent with previously published data ( $-0.65 \pm 0.09\%$ , 95% C.I., n = 8; Li et al.<sup>33</sup>). The  $\delta^{41}$ K value of the coral aragonite standard JCp-1 ( $-0.31 \pm 0.02\%$ , 2SD, n = 6) is lower than the previous values reported by Li *et al.*  $^{32,33}$  (Table 6). The varied  $\delta^{41}$ K values might reflect the heterogeneity of the reference material, which has been reported for lithium isotopes<sup>52,53</sup> and thorium isotopes. 54 The  $\delta^{41}$ K values of JDo-1 are reported for the first time. Two individual JDo-1 standards yield the same  $\delta^{41}$ K value of  $-1.00 \pm 0.01\%$  (2SD, n = 6) within our analytical precision. We also report the  $\delta^{41}$ K value of an in-house carbonate sample, South China Sea dolostone. Three individual experiments on one dolostone sample yield indistinguishable K isotope values, proving the robustness of our method in applications on natural carbonate samples.

#### Conclusion

We present the results of a series of experiments that optimize the dual-column chromatography to purify K for high-precision isotope analysis in carbonate materials using MC-ICP-MS. Our method can isolate K from 100–150 mg chemically diverse carbonate samples with satisfactory yield ( $\sim$ 100%) and negligible total blank (29.5  $\pm$  4.4 ng). Finally, we report K isotope compositions in carbonate reference materials NIST SRM 1d (limestone), JCp-1 (coral), JDo-1 (dolostone), and an in-house dolostone sample, in addition to a common silicate reference BHVO-2 for inter-laboratory comparison. Both NIST SRM 1d and BHVO-2  $\delta^{41}{\rm K}$  results agree well with published data, whereas a lower JCp-1  $\delta^{41}{\rm K}$  value may be caused by the heterogeneity of this reference material. Here we first report the  $\delta^{41}{\rm K}$  value of -1.00% in the dolomite standard JDo-1. The developed K purification method facilitates the application of K isotopes in marine carbonates for future geochemical and paleoceanographic research.

#### **Author contributions**

X.-K. Wang was responsible for the conceptualization, investigation, and writing the original draft. X.-M. Liu is responsible for the conceptualization, funding acquisition, supervision, and writing, reviewing, and editing of the manuscript. H. Chen is responsible for the investigation, manuscript writing, reviewing, and editing.

#### Conflicts of interest

There are no conflicts to declare.

## Acknowledgements

The authors acknowledge the funding support from the NSF Career Award (EAR-1848153) to X.-M. Liu, the Martin Research Fellowship from the University of North Carolina at Chapel Hill to X.-K. Wang. We thank Joseph G. Carter, Cheng Cao, and Xiao-Feng Liu for providing the samples, and Wenshuai Li for helpful discussions and comments on earlier drafts. We also thank two anonymous reviewers for thorough and constructive reviews, and the editor for handling the manuscript.

#### References

- 1 E. D. Goldberg, J. Chem. Educ., 1958, 35, 113-115.
- 2 J. Sardans and J. Peñuelas, Glob. Ecol. Biogeogr., 2015, 24, 261–275.
- 3 A. Y. Mulkidjanian, A. Y. Bychkov, D. V. Dibrova, M. Y. Galperin and E. V. Koonin, *Proc. Natl. Acad. Sci. U. S. A.*, 2012, **109**, 820–830.
- 4 M. W. Szczerba, D. T. Britto and H. J. Kronzucker, *J. Plant Physiol.*, 2009, **166**, 447–466.
- 5 W. Li, X.-M. Liu, Y. Hu, F.-Z. Teng, Y.-F. Hu and O. A. Chadwick, *Geoderma*, 2021, **400**, 115219.
- 6 N. J. W. Clipson and D. H. Jennings, Mycol. Res., 1990, 94, 1017–1022.
- 7 R. L. Rudnick and S. Gao, *Composition of the Continental Crust*, Elsevier Ltd., 2nd edn, 2013, vol. 4.
- 8 F. Culkin and R. A. Cox, *Deep-Sea Res. Oceanogr. Abstr.*, 1966, 13, 789–804.

**JAAS** Paper

- 9 N. M. Johnson, G. E. Likens, F. H. Bormann and R. S. Pierce, Geochim. Cosmochim. Acta, 1968, 32, 531-545.
- 10 F.-Z. Teng, Y. Hu, J.-L. Ma, G.-J. Wei and R. L. Rudnick, Geochim. Cosmochim. Acta, 2020, 278, 261-271.
- 11 S. Li, W. Li, B. L. Beard, M. E. Raymo, X. Wang, Y. Chen and J. Chen, Proc. Natl. Acad. Sci. U. S. A., 2019, 116, 8740-8745.
- 12 H. Chen, X.-M. Liu and K. Wang, Earth Planet. Sci. Lett., 2020, 539, 116192.
- 13 W. Li, X.-M. Liu, K. Wang and P. Koefoed, Chem. Geol., 2021, 568, 120142.
- 14 P. Michalopoulos and R. C. Aller, Science, 1995, 270, 614-
- 15 F. T. Mackenzie and R. M. Garrels, Am. J. Sci., 1966, 264, 507-525.
- 16 D. P. Santiago Ramos, L. E. Morgan, N. S. Llovd and J. A. Higgins, Geochim. Cosmochim. Acta, 2018, 236, 99-120.
- 17 W. Li, X.-M. Liu, Y. Hu, F.-Z. Teng and Y. Hu, Geochim. Cosmochim. Acta, 2021, 304, 160-177.
- 18 S. Bloch and J. L. Bischoff, Geology, 1979, 7, 193-196.
- 19 R. Hart, Earth Planet. Sci. Lett., 1970, 9, 269-279.
- 20 H. Liu, Y.-Y. Xue, G. Zhang, W.-D. Sun, Z. Tian, B. Tuller-Ross, K. Wang (and), Geochim. Cosmochim. Acta, 2021, 311, 59-73.
- 21 X.-Y. Zheng, B. L. Beard, M. Neuman, M. F. Fahnestock, J. G. Bryce and C. M. Johnson, Earth Planet. Sci. Lett., 2022, **593**, 117653.
- 22 D. P. Santiago Ramos, L. A. Coogan, J. G. Murphy and J. A. Higgins, Earth Planet. Sci. Lett., 2020, 541, 116290.
- 23 M. Hille, Y. Hu, T.-Y. Huang and F.-Z. Teng, Sci. Bull., 2019, 64, 1740-1742.
- 24 K. Wang, H. G. Close, B. Tuller-Ross and H. Chen, ACS Earth Space Chem., 2020, 4, 1010-1017.
- 25 K. Wang and S. B. Jacobsen, Geochim. Cosmochim. Acta, 2016, **178**, 223-232.
- 26 B. Tuller-Ross, B. Marty, H. Chen, K. A. Kelley, H. Lee and K. Wang, Geochim. Cosmochim. Acta, 2019, 259, 144-154.
- 27 K. Wang, W. Li, S. Li, Z. Tian, P. Koefoed and X.-Y. Zheng, Geochemistry, 2021, 81, 125786.
- 28 X. Zhou, Y. Rosenthal, L. Haynes, W. Si, D. Evans, K.-F. Huang, B. Hönisch and J. Erez, Geochim. Cosmochim. Acta, 2021, 305, 306-322.
- 29 Y. Rosenthal, E. A. Boyle and N. Slowey, Geochim. Cosmochim. Acta, 1997, 61, 3633-3643.
- 30 X.-M. Liu, L. C. Kah, A. H. Knoll, H. Cui, C. Wang, A. Bekker and R. M. Hazen, Nat. Commun., 2021, 12, 1-7.
- 31 H. Jurikova, M. Gutjahr, K. Wallmann, S. Flögel, V. Liebetrau, R. Posenato, L. Angiolini, C. Garbelli, U. Brand, M. Wiedenbeck and A. Eisenhauer, Nat. Geosci., 2020, 13, 745-750.
- 32 W. Li, X.-M. Liu, K. Wang, F. J. Fodrie, T. Yoshimura and Y.-F. Hu, Geochim. Cosmochim. Acta, 2021, 304, 364-380.
- 33 W. Li, X.-M. Liu, K. Wang, Y. Hu, A. Suzuki and T. Yoshimura, Earth Planet. Sci. Lett., 2022, 581, 117393.

- 34 X.-Y. Zheng, X.-Y. Chen, W. Ding, Y. Zhang, S. Charin and Y. Gérard, J. Anal. At. Spectrom., 2022, 37, 1273-1287.
- 35 X. Li, G. Han, Q. Zhang and Z. Miao, J. Anal. At. Spectrom., 2020, 35, 1330-1339.
- 36 X. Li and G. Han, J. Anal. At. Spectrom., 2021, 36, 676-684.
- 37 W. Li, B. L. Beard and S. Li, J. Anal. At. Spectrom., 2016, 31, 1023-1029.
- 38 Y. Hu, X.-Y. Chen, Y.-K. Xu and F.-Z. Teng, Chem. Geol., 2018, 493, 100-108.
- 39 C. Huang, H.-O. Gu, H. Sun, F. Wang and B. Chen, Spectrochim. Acta, Part B, 2021, 181, 106232.
- 40 R. H. James and M. R. Palmer, Chem. Geol., 2000, 166, 319-326.
- 41 W. Li, X.-M. Liu and L. V. Godfrey, Geostand. Geoanal. Res., 2019, 43, 261-276.
- 42 M. Humayun and R. N. Clayton, Geochim. Cosmochim. Acta, 1995, 59, 2115-2130.
- 43 H. Chen, Z. Tian, B. Tuller-Ross, R. L. Korotev and K. Wang, J. Anal. At. Spectrom., 2019, 34, 160-171.
- 44 X.-F. Liu, S. Zhai, X.-K. Wang, X. Liu and X.-M. Liu, Minerals, 2022, 12, 578.
- 45 C. Cao, X.-M. Liu, C. P. Bataille and C. Liu, Chem. Geol., 2020, 532, 119413.
- 46 K. P. Jochum, U. Nohl, K. Herwig, E. Lammel, B. Stoll and A. W. Hofmann, Geostand. Geoanal. Res., 2005, 29, 333-338.
- 47 H. Chen, N. J. Saunders, M. Jerram and A. N. Halliday, Chem. Geol., 2021, 578, 120281.
- 48 H. Liu, K. Wang (, ), W.-D. Sun, Y. Xiao, Y.-Y. Xue and B. Tuller-Ross, Geochim. Cosmochim. Acta, 2020, 277, 206-223.
- 49 F. W. E. Strelow, R. Rethemeyer and C. J. C. Bothma, Anal. Chem., 1965, 37, 106-111.
- 50 C. M. Davies, Determination of distribution coefficients for cation exchange resin and optimisation of ion exchange chromatography for chromium separation for geological materials, University of Manchester, 2012.
- 51 P. A. Sossi, G. P. Halverson, O. Nebel and S. M. Eggins, Geostand. Geoanal. Res., 2014, 39, 129-149.
- 52 L. Bastian, N. Vigier, S. Reynaud, M. E. Kerros, M. Revel and G. Bayon, Geostand. Geoanal. Res., 2018, 42, 403-415.
- 53 G. Zhu, J. Ma, G. Wei and L. Zhang, Front. Chem., 2020, 8(557489).
- 54 Y. Watanabe and S. Nakai, Geochem. J., 2006, 40, 537-541.
- 55 E. W. E. Strelow, F. Von and C. H. S. W. Weinert, Anal. Chim. Acta, 1970, 50, 399-405.
- 56 W. Li, B. L. Beard and S. Li, J. Anal. At. Spectrom., 2016, 31, 1023-1029.
- 57 L. E. Morgan, D. P. Santiago Ramos, B. Davidheiser-Kroll, J. Faithfull, N. S. Lloyd, R. M. Ellam and J. A. Higgins, J. Anal. At. Spectrom., 2018, 33, 175-186.
- 58 F. Moynier, Y. Hu, K. Wang, Y. Zhao, Y. Gérard, Z. Deng, J. Moureau, W. Li, J. I. Simon and F.-Z. Teng, Chem. Geol., 2021, 571, 120144.